Uncertainty Estimation for Kinematic Laser Tracker Measurements

Thomas Ulrich
Geodetic Institute (GIK)
Karlsruhe Institute of Technology (KIT), Germany.
Email: thomas.ulrich@kit.edu

***Abstract*—Laser trackers are widely used to measure kinematic tasks such as tracking robot movements.**

Common methods to evaluate the uncertainty in the kinematic measurement include approximations specified by the manufacturers, various analytical adjustment methods and the Kalman filter. In this paper a new, real-time technique is proposed, which estimates the 4D-path (3D-position + time) uncertainty of an arbitrary path in space. Here a hybrid system estimator in conjunction with kinematic measurement model is applied. This method can be applied to processes, which include various types of kinematic behaviour, constant velocity, variable acceleration or variable turn rates.

The new approach is compared with the Kalman filter and a manufacturer's approximations. The comparison was made using data obtained by tracking an industrial robot's tool centre point (TCP) with a Leica laser tracker AT901. It shows that the new approach is more appropriate to analysing kinematic processes than the Kalman filter, as it reduces overshoots and decreases the estimated variance. In comparison with the manufacturer's approximations, the new approach takes account of kinematic behaviour, with an improved description of the real measurement process and a reduction in estimated variance. This approach is therefore well-suited to the analysis of kinematic processes with unknown changes in kinematic behaviour.

***Keywords-component;* Laser tracker; kinematic measurement; hybrid system estimator IMM / RMIMM; uncertainty estimation; Bayesian filtering**

I. Introduction

Laser trackers have been widely and successfully used to calibrate industrial robots for many years. The most common calibration method is the static technique which means that the robot moves from point to point, pausing at each to enable calibration measurements to be made. In contrast, during a kinematic technique (often loosely called "dynamic robot calibration") the robot does not pause at calibration points and this can save a lot of time. But to apply a kinematic calibration method, the kinematic uncertainty of the measuring process as well as the dynamic model of the robot have to be known.

In addition to robot calibration, there is another important class of application which would benefit from this knowledge. This is free-form surface scanning in which a laser line scanner is kinematically tracked as it is moved over a surface to be measured. Both applications lead to the question: What is the uncertainty in a trajectory measured kinematically by laser tracker?

The laser tracker itself is a measurement device, which follows a moving reflector and measures its 3D position in spherical coordinates. Distance to the reflector is measured by interferometer (IFM) or absolute distance meter (ADM) and two optical angle encoders measure the direction to the reflector. The retro-reflector returns the outgoing laser beam back to the tracker where part of the return beam is directed onto a position sensing device (PSD). Any lateral movement of the reflector generates an offset signal at the PSD which is used in a control loop to automatically point the laser beam back to the centre of the reflector and to improve the angle encoder readings. In a first approximation, Cartesian values of a laser tracker 3D point can be calculated from the distance and angle measurements as follows.

$$\begin{aligned} x &= d * cos(\theta) * sin(\phi) \\ y &= d * sin(\theta) * sin(\phi) \\ z &= d * cos(\phi), \end{aligned} \tag{1}$$

where θ denotes the yaw angle, ϕ the pitch angle and d the distance, compare with fig. 1. The angle and distance parameters in (1) are not raw measurement values from the encoders but are modified to account for other design parameters in the laser tracker. Some current laser tracker designs are shown in fig. 3.

For the analysis presented in this paper the kinematic uncertainty of a Leica Laser Tracker AT901 was investigated. An industrial robot was used to move a cat's-eye retro-reflector with constant velocity over a predefined 3D trajectory. During the experiment, laser tracker measurements were triggered by an external source. The internal control loop of the laser tracker under test operates at a constant frequency of 3000 Hz. As a part of this loop, the PSD outputs, the angle encoders readings and the distances are stored with an associated timestamp. These timestamps are generated at a frequency of 1 MHz and therefore have a resolution of 1 µs. They are used to interpolate measurements to match the timing of the trigger impulse so that trigger impulse does not interrupt the normal measuring process of the laser tracker. The final 3D point values are therefore based on interpolated elements and are sent to an application at an frequency of 4 Hz [1],[2].

II. Kinematic Measurement

The term "kinematic measurement" can be interpreted in different ways, as shown in [3]. In this paper, a kinematic laser tracker measurement is considered as a spatiotemporal measurement of a moving reflector, hence the result can be linked via the time axis with other measurements.

978-1-4673-1954-6/12/$ 31.00 ©2012 IEEE

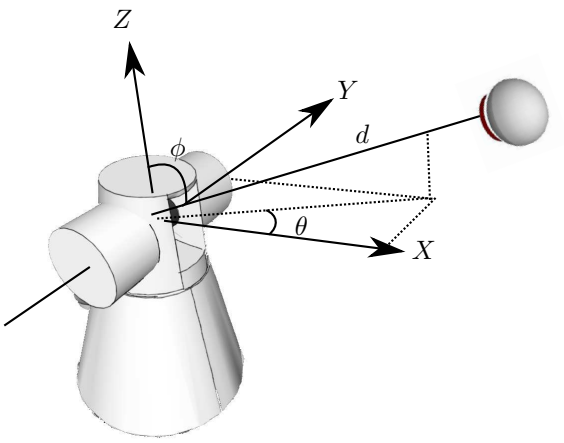

Figure. 1. Common laser tracker

There are a number of existing methods for different applications which can be used to analyse such kinematic measurements. For example, [4] suggests adjustment method in a post processing analysis and [5] suggests a Kalman Filter as a real time method, but with some restrictions. Amongst other issues, the probabilistic system model of the kinematic process must be known and all error terms must have a Gaussian distribution. To detect periodic patterns, a time series analysis was suggested by [3]. However, none of the suggested techniques is able to describe the 4D path uncertainty of an arbitrary path in a real-time application which may have different kinematic characteristics such as constant velocity, different accelerations or variable turn rates.

In order to improve the analysis of laser tracker data it is possible to utilize the state-space approach to modelling dynamic systems. Here a dynamic system is one, which changes its state over time. This approach focuses on the state vector of the system which is under investigation. The state vector is made up of all relevant information descriptive of the system, such as position sequences. In the case of a spatial tracking problem, the information is related to the kinematic characteristics of the moving reflector. The reflector, together with the laser tracker, can therefore be seen as a dynamic system, which can be analysed with Bayesian filters. If the kinematic characteristic of the path is not known in advanced, this problem can be considered as a state estimation problem of a hybrid system. In this case estimation is required of the combination of the continuous state vector as well as the discrete model. The discrete model reflects kinematic characteristics, for example if the reflector moves at constant velocity or on a curve, or if it is accelerating. Hybrid systems have been extensively studied in the field of air traffic control [6],[7],[8],[9] autonomous vehicles and driving assistance systems [10].

In the current paper the analysis is based on Bayesian filtering and a hybrid system estimator to both estimate kinematic uncertainty and to improve it. The analyzed task is the kinematic measurement of industrial robot and this analysis is compared with the common alternative methods mentioned above.

III. Bayesian Filtering

The kinematic laser tracker measurement of a moving reflector can be viewed as a dynamic system. To analyse a dynamic system with the Bayesian filter approach two models are required:

- A system model that describes the evolution of the system over time.
- A measurement model relating the noisy data measurements to the state.

If these models are available in a probabilistic form, the state space formulation is ideally suited to the application of Bayesian filters [11].

A Bayes filter calculates, a posterior, the probability distribution over the state vector $\boldsymbol{x}_t$ at time t based on all past measurements $\boldsymbol{z}_{1:t}$ and all past control inputs of the system model $\boldsymbol{u}_{1:t}$. In general a Bayes filter consists of a prediction step and an update step. The prediction step at time t calculates a prior probability density function (pdf) using a system model and requires the pdf $p\left(\boldsymbol{x}_{t-1}|\boldsymbol{z}_{1:t-1}\right)$. As described in [12] the prior pdf can be calculated by

$$p\left(\boldsymbol{x}_t|\boldsymbol{z}_{1:t-1},\boldsymbol{u}_{1:t}\right) = \int p\left(\boldsymbol{x}_t|\boldsymbol{x}_{t-1},\boldsymbol{u}_t\right) p\left(\boldsymbol{x}_{t-1}|\boldsymbol{z}_{1:t-1},\boldsymbol{u}_{1:t-1}\right) dx_{t-1} \quad (2)$$

The update step calculates the required posterior as follows

$$p\left(\boldsymbol{x}_t|\boldsymbol{z}_{1:t},\boldsymbol{u}_{1:t}\right) = \frac{p\left(\boldsymbol{z}_t|\boldsymbol{x}_t\right) p\left(\boldsymbol{x}_t|\boldsymbol{z}_{1:t-1},\boldsymbol{u}_{1:t}\right)}{p\left(\boldsymbol{z}_t|\boldsymbol{z}_{1:t-1},\boldsymbol{u}_{1:t}\right)} \quad (3)$$

Within the update step the current measurements $\boldsymbol{z}_t$ modify the prior pdf depending on the likelihood function, which is defined by the measurement model. For the derivation of the Bayes filter the assumption is made, that the state $\boldsymbol{x}_t$ is a first-order Markov chain. The variance of the resulting pdf after the update step can be seen as an kinematic uncertainty, as it includes all influences of measuring process as well as the system process.

A standard kinematic laser tracker measurement can be seen as a tracking problem, in which the system model is not known and must be estimated. Due to the fact that the dynamic system model of the kinematic process is often not accurately known in advance, the analysis method should take several system models into account. This can be done by a hybrid system estimator approach.

A. System Model

A Kalman filter is a traditional Bayesian filter, but does not perform very well to estimate the continuous state of a reflector, because it is likely, that the model, on which the filter bases, does not accurately represent the current behaviour of the reflector at all times. Due to the unknown inputs $\boldsymbol{u}_{1:t}$ of the tracking system to the analysis, the usual approach is to include the model inaccuracies into the process noise, which reduces the accuracy of the state.

Estimation of both the continuous state and the discrete model leads to a so-called hybrid estimation problem [6]. The hybrid systems used in this paper models the continuous dynamic by difference equation and the discrete-state dynamics by a finite Markov chain.

A discrete-time stochastic hybrid system can be expressed as follows

$$\begin{aligned} \boldsymbol{x}_{t+1} &= f_t^i\left(\boldsymbol{x}_t, \boldsymbol{u}_t, w_t^i\right) \\ \boldsymbol{z}_t &= h_t^i\left(\boldsymbol{x}_t, v_t^i\right), \end{aligned} \tag{4}$$

where f^i is the system model function of model i with its system process noise w and h^i is the measurement model function of model i with its measurement noise v. The model i is governed by the finite Markov-chain

$$\mu_{t+1} = \Pi\, \mu_t, \tag{5}$$

where $\Pi = \{\pi_{ij}\} \in \mathbb{R}^{r\times r}$ is the transition probability matrix, $\mu_t \in \mathbb{R}^r$ is the model probability and r the count of models. The state estimate can be expressed as

$$\hat{\boldsymbol{x}}_{t+1} = \sum_{i=1}^{r} \hat{\boldsymbol{x}}_{t+1}^i p\left(m_{t+1}^i | \boldsymbol{z}_{1:t+1}\right), \tag{6}$$

where $\hat{\boldsymbol{x}}_{t+1}^i = \int x_{t+1} p\left(x_{t+1}|\boldsymbol{z}_{1:t+1}, m^i\right) \mathrm{d}x_{t+1}$ is the state estimate of the state $\boldsymbol{x}_{t+1}$ given the conditional probability, that the model at time $t+1$ is m_{t+1}^i and is computed by the state estimator matched to model i, based on [6]. Hence, the estimator in equation (6) can be seen as a weighted sum with the weights $p\left(m_{t+1}^i|\boldsymbol{z}_{1:t+1}\right)$, which are the model probability μ_{t+1}^i of the model i at time t_{t+1}.

The Interacting Multiple Model (IMM) filter is a widely used hybrid system estimator due to its excellent performance in comparison with other hybrid system estimators [6]. It approximates a set of possible system models and calculates a combination over all implemented models [8]. Possible models of reflector manoeuvres can therefore be defined in advance, depending on the expected kinematic process. In an IMM filter, the implemented models can also have state vectors with different dimensions. The author of [6] have proposed an improvement to the IMM-filter called Residual-Mean Interacting Multiple Model (RMIMM). They have shown, that the model estimation delay of a RMIMM filter is slightly better than the one of an IMM filter. The different between the IMM and the RMIMM is in the way in which weights are calculated for equation (6) to reduce the false model estimation. This is achieved by increasing the different between the likelihood of the correct model and the others.

The combination of the different models is made according to a general Markov model for the transition between the states. An IMM / RMIMM filter consists of a bank of r parallel Bayesian filters and a transition matrix, which defines the transition probability between the states of each model [7]. These filters are usually made up of a range of system models, which are deployed by different Bayesian filters like a Kalman– or Particle Filter [8], [13]. Three major steps are carried out in an IMM / RMIMM filter:

- Interaction/Mixing
- Filter
- Estimate and Covariance Combination

The following description of these three steps is loosely based on the derivation of [8]. For a simplified description the Kalman filter is used as an example of a Bayesian filter.

1) Interaction/Mixing Step: The interaction/mixing step, is the first step. Here the mixed inputs for each model are calculated. Assuming a Kalman filter, the mixed inputs are the means and the covariances for each filter, which can be calculated as

$$\hat{\boldsymbol{x}}_{t-1}^{0j} = \sum_{i=1}^{r} \mu_{t-1}^{i|j} \hat{\boldsymbol{x}}_{t-1}^i \qquad j = 1, \cdots, r \tag{7}$$

$$\begin{aligned} P_{t-1}^{0j} = \sum_{i=1}^{r} \mu_{t-1}^{i|j} \Big\{ P_{t-1}^i + \left[\hat{\boldsymbol{x}}_{t-1}^i - \hat{\boldsymbol{x}}_{t-1}^{0j}\right] \\ \left[\hat{\boldsymbol{x}}_{t-1}^i - \hat{\boldsymbol{x}}_{t-1}^{0j}\right]^{\mathrm{T}} \Big\} \qquad j = 1, \cdots, r \end{aligned} \tag{8}$$

where $\hat{\boldsymbol{x}}_{t-1}^i$ and P_{t-1}^i are the mean and covariance for the model i at time step $t-1$. The conditional probability $\mu_{t-1}^{i|j}$, that the system made the transition from model i to model j at time $t-1$ can be calculated as

$$\mu_{t-1}^{i|j} = \frac{1}{\overline{c}_j} \pi_{ij} \mu_{t-1}^i \qquad i, j = 1, \cdots, r \tag{9}$$

$$\overline{c}_j = \sum_{i=1}^{r} \pi_{ij} \mu_{t-1}^i \qquad j = 1, \cdots, r \tag{10}$$

where π_{ij} is the transition probability for each model m^i and m^j according to the transition probability matrix of the Markov model and $\overline{c}_j$ is normalization factor.

2) Filter Step: In this second step, the Bayesian filters are applied. Assuming Kalman filter for each model m^i then the prediction and update step are done as

$$\left[\hat{\boldsymbol{x}}_t^{-,i}, P_t^{-,i}\right] = \mathrm{KF}_p\left(\hat{\boldsymbol{x}}_{t-1}^{0j}, P_{t-1}^{0j}, A_{t-1}^i, Q_{t-1}^i\right) \tag{11}$$

$$\left[\hat{\boldsymbol{x}}_t^i, P_t^i\right] = \mathrm{KF}_u\left(\hat{\boldsymbol{x}}_t^{-,i}, P_t^{-,i}, \boldsymbol{z}_t, H_t^i, R_t^i\right) \tag{12}$$

where $\mathrm{KF}_p(\cdot)$ stands for the Kalman filter prediction step and $\mathrm{KF}_u(\cdot)$ for the Klaman filter update step. A denotes the system transition matrix and Q the system covariance matrix. Both are derived from the system model m^i. According to the measurement model H represents the measurement matrix and R the covariance matrix of the measurement model. In addition to the mean and covariance the model probability for each model m^i must be calculated.

The probability for a IMM / RMIMM filter is determined as

$$\mu_t^j = \tfrac{1}{c} \Lambda_t^j \overline{c}_j \qquad j = 1, \cdots, r \tag{13}$$

where c is the normalization constant, calculated as

$$c = \sum_{j=1}^{r} \Lambda_t^j \overline{c}_j. \tag{14}$$

Within a IMM filter the likelihood of the measurement for each model is calculated as

$$\Lambda_t^j = \mathcal{N}\left(\boldsymbol{d}_t^j; 0, S_t^j\right) \tag{15}$$

where $\boldsymbol{d}_t^j$ are the residuals of the measurements and S_t^j is the innovation covariance matrix for the model m^j in the KF

update step. The likelihood for the RMIMM filter is calculated by

$$\Lambda_t^j = \begin{cases} \frac{N_t^j \mathcal{N}\left(\boldsymbol{d}_t^j; 0, S_t^j\right)}{\sum_{i=1}^{r} N_t^i \mathcal{N}\left(\boldsymbol{d}_t^j; 0, S_t^j\right)} & \text{if } \overline{d}_t^j \neq 0 \\ \mathcal{N}\left(\boldsymbol{d}_t^j; 0, S_t^j\right) & \text{otherwise} \end{cases} \tag{16}$$

with

$$N_t^i = \begin{cases} \left\| \overline{d}_t^i \right\|^{-1} & \text{if } \overline{d}_t^j \neq 0 \\ 1 & \text{otherwise} \end{cases} \tag{17}$$

where $\overline{d}_t^j$ is the mean value of the residuals in model i at time t. The conditional likelihood Λ^j for each filter is directly comparable to the data association problem. This problem is well known by simultaneous localization and mapping (SLAM) algorithms and has been extensively investigated [14]. [6] have pointed out the a IMM filter can be improved when the difference between the likelihood values is increased. In SLAM algorithms, more features are included in an augmented state vector to obtain a greater difference between the likelihood values and so avoid ambiguities [15].

3) Estimate and Covariance Combination: In this third step, the combined state estimate and covariance are calculated as

$$\begin{aligned} \hat{\boldsymbol{x}}_t &= \sum_{j=1}^{r} \mu_t^j \hat{\boldsymbol{x}}_t^j \\ P_t &= \sum_{j=1}^{r} \mu_t^j \left\{ P_t^j + \left[\hat{\boldsymbol{x}}_t^j - \hat{\boldsymbol{x}}_t \right] \left[\hat{\boldsymbol{x}}_t^j - \hat{\boldsymbol{x}}_t \right]^{\mathrm{T}} \right\}. \end{aligned} \tag{18}$$

It can be seen, that the IMM / RMIMM filter is ideal suited to the analysis of longer kinematic measurement where more than one model exists in dynamic process. Due to the acceleration there are at least two different models, at the beginning and at the end of each kinematic movement, which is otherwise considered as a constant velocity process.

B. Measurement Model

The Bayesian filter mentioned earlier also consists of measurement model composed of a deterministic and a probabilistic model. Equation (1) can be viewed as the deterministic model and the probabilistic can be derived from it. Comparison with equation (12) reveals that this model and its covariance can change with each time step. This property is important for the analysis of kinematic laser tracker measurements, due to the fact, that a laser tracker generally consists of a range measuring device as well as two angle encoders. This means, that the uncertainty depends on the reflector's position, which changes every time step throughout a kinematic measurement. In spite of some geometrical design differences, the 3-D point variance of a laser tracker can be estimate via the uncertainty propagation as a first-order approximation over

$$\begin{aligned} \sigma_x^2 &= (\cos\theta \, \sin\phi)^2 \, \sigma_d^2 + (-d \, \sin\phi \, \sin\theta)^2 \, \sigma_\theta^2 + \\ &\quad (d \, \cos\phi \, \cos\theta)^2 \, \sigma_\phi^2 \\ \sigma_y^2 &= (\sin\theta \, \sin\phi)^2 \, \sigma_d^2 + (d \, \cos\theta \, \sin\phi)^2 \, \sigma_\theta^2 + \\ &\quad (d \, \cos\phi \, \sin\theta)^2 \, \sigma_\phi^2 \end{aligned}$$

$$\sigma_z^2 = (\cos\phi)^2 \, \sigma_d^2 + (-d \, \sin\phi)^2 \, \sigma_\phi^2, \tag{19}$$

where σ_d denotes the standard deviation of distance, σ_ϕ the standard deviation of the pitch angle and σ_θ the standard deviation of the yaw angle, see fig. 1. Equations (19) do not take into account any correlations between the axes.

In [4] the author describes the synchronization between some trigger pulses as the main source of uncertainty by kinematic measurements for the Leica laser tracker model, as the PSD control point is determined during the initialisation of the laser tracker [16]. The synchronization uncertainty is directly linked to the speed, which results in the first order approximation

$$\begin{aligned} x_k &= x + V_x \cdot t_s \\ y_k &= y + V_y \cdot t_s \\ z_k &= z + V_z \cdot t_s. \end{aligned} \tag{20}$$

Hence, a kinematic 3D variance can be expressed by

$$\begin{aligned} \sigma_{x_k}^2 &= \sigma_x^2 + t_s^2 \, \sigma_{V_x}^2 + V_x^2 \, \sigma_{t_s}^2 \\ \sigma_{y_k}^2 &= \sigma_y^2 + t_s^2 \, \sigma_{V_y}^2 + V_y^2 \, \sigma_{t_s}^2 \\ \sigma_{z_k}^2 &= \sigma_z^2 + t_s^2 \, \sigma_{V_z}^2 + V_z^2 \, \sigma_{t_s}^2, \end{aligned} \tag{21}$$

where t_s represents the synchronization error and σ_{t_s} its standard deviation. V is the velocity and σ_V its standard deviation. Here it is assumed that t_s denotes the synchronization between each trigger impulse as well as the internal synchronization between the distance measuring device and the angle encoders. Equation (20) and (21) are only valid for movement with constant velocity.

In order to describe a kinematic 3D point uncertainty also the environmental influences must also be taken into account. In equations (19) it can clearly be seen that the kinematic 3D point variance depends on position and synchronization. With a full description of the measurement model and its uncertainty, kinematic laser tracker measurements are appropriate for analysis using a Bayesian filter.

IV. Implementation

The following section describes the analysis of a kinematic laser tracker measurement using a Leica AT901 laser tracker which followed a cat's eye reflector manipulated by an industrial robot. The predefined trajectory along which the reflector was moved at a constant speed of $500\ \mathrm{mm/s}$, can be seen in fig. 5. Due to robot performance limitations, $500\ \mathrm{mm/s}$ was the maximum constant speed for this trajectory. The trajectory was defined by the edges of a cube with semicircles on its sides. The robot first moved the reflector along the edges of the cube and then around the semicircles.

A. Development of the System Model

With regard to the experiment design and the test trajectory, three system models should be considered:

- Constant velocity model
- Constant acceleration model
- Coordinated turn model

The constant velocity of the reflector is expressed in a continuous, white-noise acceleration model, where the velocity is a

Wiener process according to [8]. Hence, the state space vector of the first model is $\boldsymbol{x}^{\mathrm{I}} = [x\ \dot{x}\ y\ \dot{y}\ z\ \dot{z}]^{\mathrm{T}}$. The discrete-time state equation is expressed as

$$\begin{aligned} \boldsymbol{x}_{t+1}^{\mathrm{I}} &= \mathrm{diag}\left[F^{\mathrm{I}}, F^{\mathrm{I}}, F^{\mathrm{I}}\right] x_t + w_t^{\mathrm{I}} \\ F^{\mathrm{I}} &= \begin{bmatrix} 1 & \Delta t & 0 \\ 0 & 1 & 0 \\ 0 & 0 & 1 \end{bmatrix} \end{aligned} \tag{22}$$

with the sampling period Δt. The covariance of the discrete-time process noise w_t^{I} is

$$\begin{aligned} Q^{\mathrm{I}} &= \mathrm{diag}\left[Q_c^{\mathrm{I}}, Q_c^{\mathrm{I}}, Q_c^{\mathrm{I}}\right] \tilde{q}^{\mathrm{I}} \\ Q_c^{\mathrm{I}} &= \begin{bmatrix} \frac{1}{3}\Delta t^3 & \frac{1}{2}\Delta t^2 \\ \frac{1}{2}\Delta t^2 & \Delta t \end{bmatrix} \end{aligned} \tag{23}$$

assuming $\tilde{q}^{\mathrm{I}}$ is a constant power spectral density of the process noise.

The model with a constant acceleration is expressed as

$$\begin{aligned} \boldsymbol{x}_{t+1}^{\mathrm{II}} &= \mathrm{diag}\left[F^{\mathrm{II}}, F^{\mathrm{II}}, F^{\mathrm{II}}\right] x_t + w_t^{\mathrm{II}} \\ F^{\mathrm{II}} &= \begin{bmatrix} 1 & \Delta t & \frac{1}{2}\Delta t^2 \\ 0 & 1 & \Delta t \\ 0 & 0 & 1 \end{bmatrix} \end{aligned} \tag{24}$$

with the state vector $\boldsymbol{x} = [x\ \dot{x}\ \ddot{x}\ y\ \dot{y}\ \ddot{y}\ z\ \dot{z}\ \ddot{z}]^{\mathrm{T}}$ after [8]. Here the acceleration is a Wiener process and the covariance of the discrete-time process noise w_t^{II} is

$$\begin{aligned} Q^{\mathrm{II}} &= \mathrm{diag}\left[Q_c^{\mathrm{II}}, Q_c^{\mathrm{II}}, Q_c^{\mathrm{II}}\right] \tilde{q}^{\mathrm{II}} \\ Q_c^{\mathrm{II}} &= \begin{bmatrix} \frac{1}{20}\Delta t^5 & \frac{1}{8}\Delta t^4 & \frac{1}{6}\Delta t^3 \\ \frac{1}{8}\Delta t^4 & \frac{1}{3}\Delta t^3 & \frac{1}{2}\Delta t^2 \\ \frac{1}{6}\Delta t^3 & \frac{1}{2}\Delta t^2 & \Delta t \end{bmatrix} \end{aligned} \tag{25}$$

with the $\tilde{q}^{\mathrm{II}}$ power spectral density of the process noise.

The coordinated turn model assumes a constant turn rate ω in a navigation plane [9]. Here the turn rate is defined as the norm of the angle velocity vector $\boldsymbol{\Omega}$ and can be calculated as

$$\omega = \|\boldsymbol{\Omega}\| = \frac{|\boldsymbol{v} \times \boldsymbol{a}|}{v^2} = \frac{|\boldsymbol{v}|\,|\boldsymbol{a}|}{v^2} = \frac{a}{v} \tag{26}$$

if $\boldsymbol{\Omega} \perp \boldsymbol{v}$ [9]. Fig. 2 shows the relationship between the velocity vector $\boldsymbol{v}$ as well as the acceleration vector $\boldsymbol{a}$ in the navigation plane, to which the angle velocity vector $\boldsymbol{\Omega}$ is perpendicular. The discrete time coordinated turn model can be expressed as

$$\begin{aligned} \boldsymbol{x}_{t+1}^{\mathrm{III}} &= \mathrm{diag}\left[F^{\mathrm{III}}(\omega), F^{\mathrm{III}}(\omega), F^{\mathrm{III}}(\omega), 1\right] x_t + \Gamma w_t^{\mathrm{III}} \\ F^{\mathrm{III}}(\omega) &= \begin{bmatrix} 1 & \sin(\omega\Delta t)/\omega & (1-\cos(\omega\Delta t))/\omega^2 \\ 0 & \cos(\omega\Delta t) & \sin(\omega\Delta t)/\omega \\ 0 & -\omega\sin(\omega\Delta t) & \cos(\omega\Delta t) \end{bmatrix} \\ \Gamma &= \begin{bmatrix} 0 & 0 & 1 & 0 & 0 & 0 & 0 & 0 & 0 & 0 \\ 0 & 0 & 0 & 0 & 0 & 1 & 0 & 0 & 0 & 0 \\ 0 & 0 & 0 & 0 & 0 & 0 & 0 & 0 & 1 & 0 \\ 0 & 0 & 0 & 0 & 0 & 0 & 0 & 0 & 0 & 1 \end{bmatrix} \end{aligned} \tag{27}$$

with the augmented state vector $\boldsymbol{x} = [x\ \dot{x}\ \ddot{x}\ y\ \dot{y}\ \ddot{y}\ z\ \dot{z}\ \ddot{z}\ \omega]^{\mathrm{T}}$, based on [9].

The three system models should be sufficient to model the kinematic process of the robot in hybrid system estimator without loosing accuracy as in a Kalman filter, which considers only one model. In the hybrid estimator, curves, the constant velocities as well as the accelerations between each period, are taken into consideration.

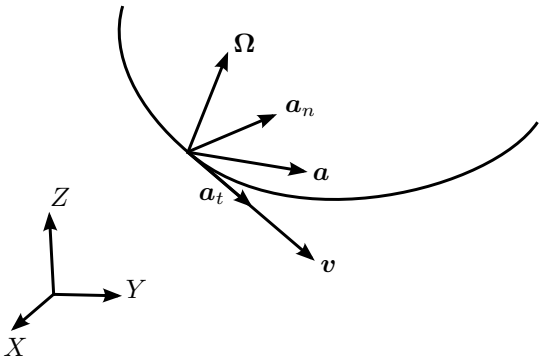

Figure. 2. Coordinated turn model.

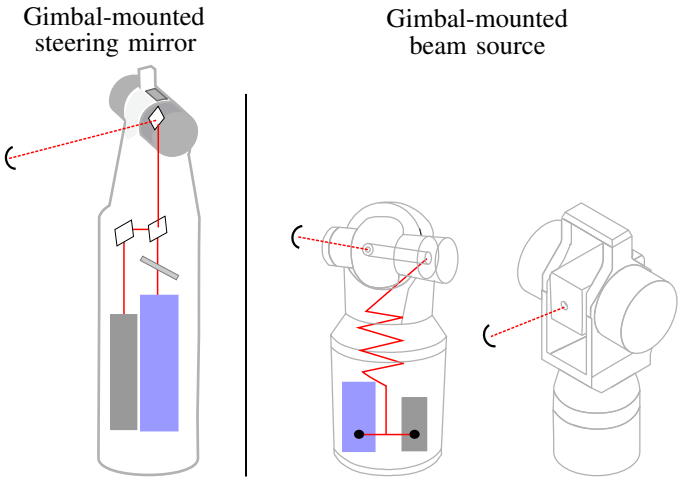

Figure. 3. Different design types of laser trackers, either with a gimbal-mounted beam steering mirror or with a gimbal-mounted beam source.

B. Development of the Measurement Model

In general, commercial laser trackers can be assigned to one of two classes depending on design. There are laser trackers

- with a gimbal-mounted beam steering mirror and
- with a gimbal-mounted beam source.

Fig. 3 shows examples of different types of a laser tracker. Calibration models have been published for both types of laser trackers. A geometrical alignment model for the gimbal-mounted beam source is presented in [17] and in [18]. The Leica laser tracker AT901 belongs to the first group. All these models describe only the geometrical alignment parameters. These are not sufficient to calculate a precise probability density function of a moving reflector which can be used in a Bayesian filter algorithm, as they do not take into account environmental and kinematic influences.

To develop a measurement model for a trajectory measured kinematically by a Leica laser tracker AT901, the model

described in [19] is augmented by additional terms which represent kinematic as well as the environmental effects. A group of 16 parameters are used in the geometrical alignment model described in [19]. These parameters are:

- Transit axes offset e
- Mirror offset f
- Beam offset $O1x$ $O1y$
- Cover plate offset $O2x$ $O2y$
- Mirror tilt c
- Transit axis tilt, i
- Beam axis tilt Ix Iy
- Yaw angle encoder eccentricity Ex Ey
- Pitch angle encoder eccentricity Kx Ky
- Pitch angle offset j
- Distance parameter k.

This model is valid in both static and kinematic measurement, but for kinematic measurement additional parameters must be taken into consideration. A corrected value for the yaw angle θ_{c}, the pitch angle ϕ_{c} and the distance d_{c} can be calculated with these parameters and the correction equations of [19] using the following:

$$\begin{aligned} \theta_c &= f_{\text{yaw}}\left(\boldsymbol{h}_\theta\right) \\ \phi_c &= f_{\text{pitch}}\left(\boldsymbol{h}_\phi\right) \\ d_c &= f_{\text{distance}}\left(\boldsymbol{h}_d\right) \end{aligned} \tag{28}$$

where $\boldsymbol{h}$ are parameter vectors containing the parameter for the correction functions f of the yaw angle θ, the pitch angle ϕ and the distance d.

To take environmental influences into account, the distance $dist_c$ must be additionally corrected with the formulas according to [20], which depend on

- the temperature,
- the air pressure,
- the relative humidity,
- the wave length of the laser source and
- the measured distance.

If these parameters are stored in a vector $\boldsymbol{h}_{meteo}$ the meteorology correction can be expressed in brief as

$$d_{\acute{c}} = f_{meteo}\left(\boldsymbol{h}_{meteo}, d_c\right). \tag{29}$$

To apply the equations (29), it is assumed that these represent the current refractive index along the tracker's laser beam. After applying the full correction process a static 3D point can be calculated with the equations (1) as

$$\begin{aligned} x &= d_{\acute{c}} * \cos\left(\theta_c\right) * \sin\left(\phi_c\right) \\ y &= d_{\acute{c}} * \sin\left(\theta_c\right) * \sin\left(\phi_c\right) \\ z &= d_{\acute{c}} * \cos\left(\phi_c\right). \end{aligned} \tag{30}$$

Assumption that one delay time includes the delay time for each component, i.e. the distance and the angle encoders readings, a kinematic 3D point can be determined with

$$\begin{aligned} x_k &= d_{\acute{c}} * \cos\left(\theta_c\right) * \sin\left(\phi_c\right) + v_x t_s + 1/2\ a_x t_s^2 \\ y_k &= d_{\acute{c}} * \sin\left(\theta_c\right) * \sin\left(\phi_c\right) + v_y t_s + 1/2\ a_y t_s^2 \\ z_k &= d_{\acute{c}} * \cos\left(\phi_c\right) + v_z t_s + 1/2\ a_z t_s^2 \end{aligned} \tag{31}$$

where v expresses the speed and a the acceleration for each axis and t_s the synchronization error.

The equations (28) to (31) describe a deterministic model of a Leica laser tracker. However, a measurement model for a Bayesian filter consists additionally of a probabilistic model. This can be deduced with the variance propagation or with the Monte Carlo Method [21]. For complex functions it is simpler to use the Monte Carlo Method instead of the variance propagation. In addition, the Monte Carlo Method avoid linearisation errors [12]. Equations (31), in combination with the Monte Carlo Method, can be interpreted as a kinematic virtual laser tracker (kVLT) which determines the probability density for any arbitrary point by applying 30 critical parameters. For normal users it is not possible to get the PSD values during tracking and so the angle standard deviation has to be adjusted to include the behaviour of the PSD sensor. As equations (29) do not consider a 3D refraction index, the angle encoder readings must be further modified.

C. Combining within an IMM Filter

To implement the measurement model and the different system models as described in IV-A, a Bayesian filter type must be chosen. Specific details about the different types of Bayesian filter can be found in [12] and [22]. This decision depends on the model type, linear or non-linear, the distribution of the parameter and the approximation error. The extended Kalman filter were chosen in [8] for the non-linear coordinated turn model and the Kalman filter for a constant velocity model. Whereas in [13] the particle filter was used for all model types.

For all filters in the filter bank, it is assumed, that the laser tracker is always the same, which measurement model is known, and the measurement are normal distributed.The filter update equation (12) can be rewritten as

$$\left[\hat{\boldsymbol{x}}_t^i, P_t^i\right] = \text{KF}_u\left(\hat{\boldsymbol{x}}_t^{-,i}, P_t^{-,i}, \boldsymbol{z}_t, H_t, R_t^i\right) \tag{32}$$

As can be seen from equation (21), the kinematic variance of a point is dependent on the velocity and its variance. Estimated velocity and its variance are different for the different filter models. The laser tracker model of equation (31) is used to determine for each time instance t a covariance matrix R_t^i as follows

$$R_t^i = E\left(\left[\boldsymbol{x}_r - \overline{\boldsymbol{x}}_r\right]\left[\boldsymbol{x}_r - \overline{\boldsymbol{x}}_r\right]^{\text{T}}\right), \tag{33}$$

where $\boldsymbol{x}_r$ is the state vector of $(x_k\ y_k\ z_k)$ and containing the individual random variables according to the Monte Carlo Method of equation (31).

Due to the assumption of a normally distributed measurements, the linear constant velocity model and constant acceleration model are implemented in a Kalman filter, whereas the non-linear coordinated turn model is implemented in an Unscented Kalman filter. To achieve a higher accuracy the Unscented Kalman filter is chosen instead of the Extend Kalman filter. The unscented transformation is more accurate for the propagation of the means and the covariances than the linearisation, which is used by an Extended Kalman filter, shown in [12] and [22]. As described in [12], the Unscented Kalman filter is more convenient to use as the Particle Filter, if the underlying distribution is approximately a normal

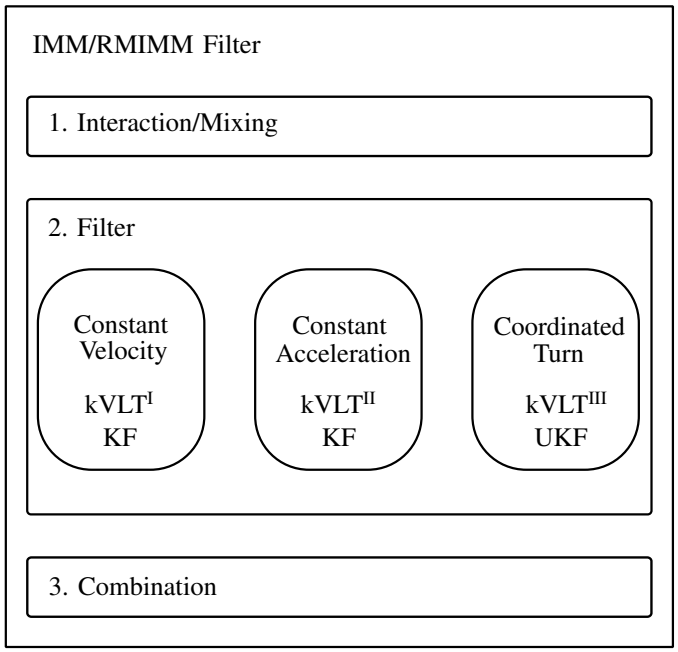

Figure. 4. Implemented IMM / RMIMM filter with the different typical steps. The non-linear model is described by an Unscented Kalman filter (UKF), whereas the other linear models are described by a normal Kalman filter (KF).

	Anderson-Darling	Lilliefors
normal distributed [%]	95.07	94.90

TABLE I
NORMAL DISTRIBUTION TEST

distribution. The implemented IMM / RMIMM filter is shown in fig. 4. Due to the normal distribution the implemented IMM / RMIMM can be seen as a Gaussian sum filter.

V. RESULTS

To determine if the measurement model can be considered as normally distributed, two different test were made. The first test is the Anderson-Darling test and the second one is the Lilliefors test. Results are shown in table I. The Lilliefors test based on the well known Kolmogorov-Smirnov test, but in contrast to the Kolmogorov-Smirnov test, the Lilliefors test can be applied even if the mean and covariance are unknown, as described in [23]. For comparison, the Anderson-Darling test was also applied. This is based on different statistics from the Kolmogorov-Smirnov test and gives a better performance [24].

For both tests, 7900 data points along the test trajectory, as shown in fig. 5 were used in conjunction with the Monte-Carlo method applied to equation (31) with 5000 samples. The significant level α was set to 0.05 for both test. Both tests show that the measurement model can be taken as normally distributed. It is therefore justifiable to use the Kalman and Unscented Kalman filter in a hybrid system model for the further analysis, as suggested previously.

To compare the new analysis methods, i.e. the RMIMM filter and the IMM filter, against more commonly used methods, i.e. the specification of Leica and the Kalman Filter, all methods were tested with the same data set.

The kinematic accuracy for a Leica Laser Tracker LTD500 is specified with $\pm\ 20 - 40\ \mu\mathrm{m/m}$, in [25], [1]. According to [26] this specification can also be applied to the Leica Laser Tracker AT901. Taking account of the reflector's relatively slow speed of approximately $500\ \mathrm{mm/s}$, compared with the tracker's maximum tracking speed of $6\ \mathrm{m/s}$, the lower bound of $20\ \mu\mathrm{m/m}$ was chosen for the analysis. The results of this specification are shown in fig. 5a, the range dependency is clearly visible. For the commonly used Kalman filter method, suggested in [5], the Leica specification was used as the measurement model. The results of the Kalman filter method are shown in fig. 5b. As expected, the standard deviation drops significant from minimum $92\ \mu\mathrm{m}$ to $55\ \mu\mathrm{m}$, but it is also clear that the variances were set to very large values to cover the inaccuracy of the applied model. This effect has already been mentioned in section III Bayesian Filtering.

To improve the Kalman filter method, the RMIMM filter and IMM filter were applied to the data set. Fig. 6 shows the results and there is no noticeable difference between them. Due to the slow speed of the experiment and the nearly still stand at the model change points at the corners, the advantage of a faster model detection of the RMIMM filter instead to the IMM filter cannot be seen. In contrast, the difference between the commonly used methods in fig. 5, and hybrid algorithm methods in fig. 6 is obvious. With the coordinated turn model, the hybrid filters are also capable of dealing with cross-track deviations of the robot. They are also sensitive to the low standard deviation of laser tracker measurement, which is not the case with the more common Kalman filter. The clear range dependency shows that the speed of $500\ \mathrm{mm/s}$ is too slow, so the alignment errors and range dependency overlap the kinematic uncertainty effects. Otherwise there must be significant lower standard deviation at the corners, where the speed drops nearly to zero in order to change direction of movement as can be seen from fig. 7. The higher range dependency at slower speeds emphasizes the importance of reliable static laser tracker models, assuming the delay time can be taken as $\pm\ 5\ \mu\mathrm{s}$ as claimed in [2] and [4]. Specifying a delay time of zero could be justified by the post-processing interpolation step, as discussed in section I Introduction.

Another advantage of the hybrid algorithms is, that they avoid overshoots, which not only generate poor standard deviation but also slightly wrong state estimates. As expected, these overshoots are found at path corners where the system model changes. One example of these overshoots is shown in fig. 8. Hybrid algorithms successfully prevent overshoots, due to their fast model detection. There is no occurrence of overshoots where the RMIMM filter generates a faster model detection than the IMM filter. In addition fig. 8 shows, that there were no clear model change points at every corner. The robot makes a small loop instead of a curve or sharp edge, which leads to many more model changes than expected and ultimately to calculation of a higher standard deviation by the hybrid algorithms.

To compare all analysis methods, their mean standard deviation were calculated and listed in table II. One can see that the

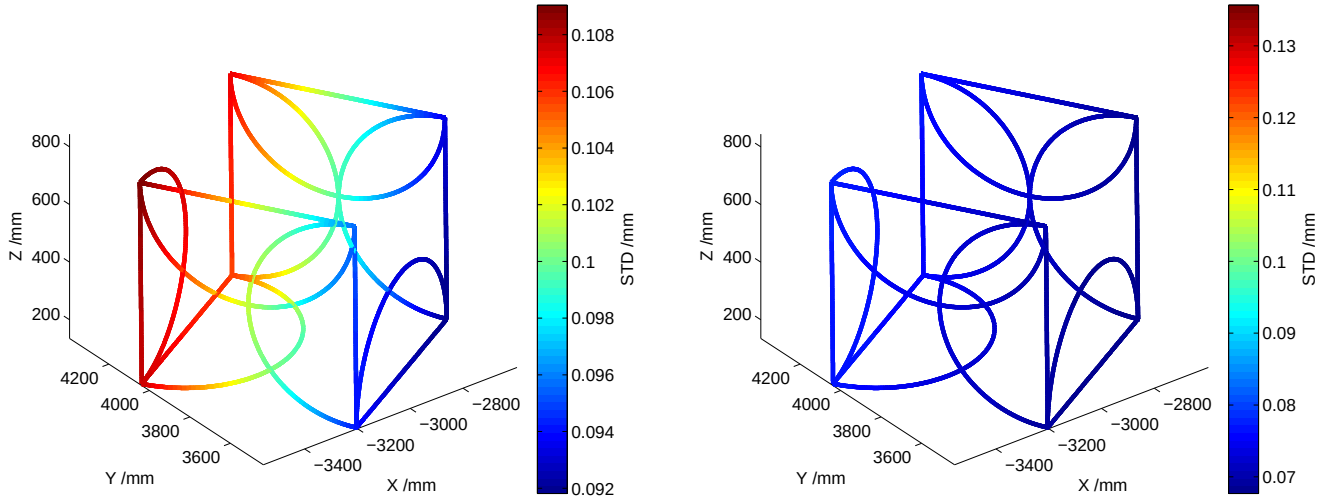

(a) Approximation

(b) Kalman filtering

Figure. 5. Standard analysis methods.

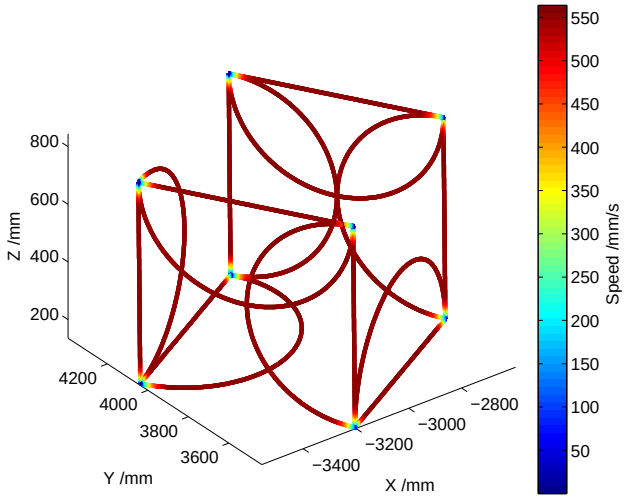

Figure. 7. The reached speed for each point of the experiment.

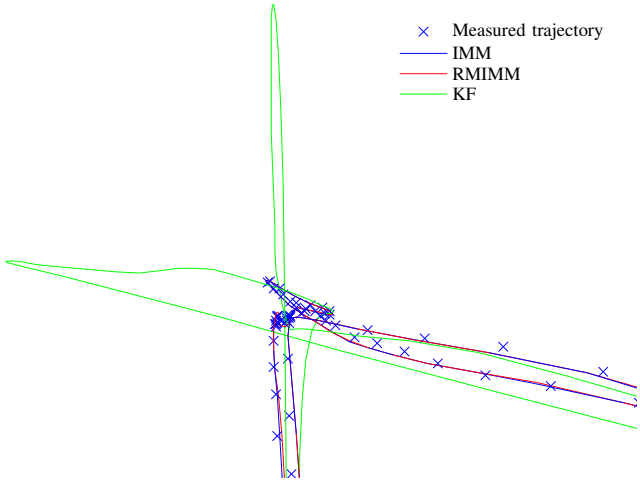

Figure. 8. Over shoots provided through the Kalman filter in comparison with the estimation of the hybrid filter algorithms.

	RMIMM	IMM	Approx.	KF
Mean standard deviation [mm]	0.0243	0.0239	0.1019	0.0735

TABLE II
COMPARISON BETWEEN THE ANALYSIS METHODS

IMM filter delivers the smallest mean standard deviation with 0.0239 mm, only slightly different to the RMIMM filter result. This is depended on the long still stand time at the beginning and at the end of the experiment. During these period, small movements of the robot were interpreted as model changes by the RMIMM filter which provided a higher standard deviation as a result. It can be seen, therefore, that the hybrid filters deliver roughly a 4 times better standard deviation than the approximation of the manufacture and a 3 times better than common Kalman filter approach.

VI. Conclusion

In the presented example of a robot following a trajectory at constant speed, it has been shown that its analysis as a hybrid system can provide an estimation of the paths uncertainty. Due to the slow speed adopted in the test, it was not possible

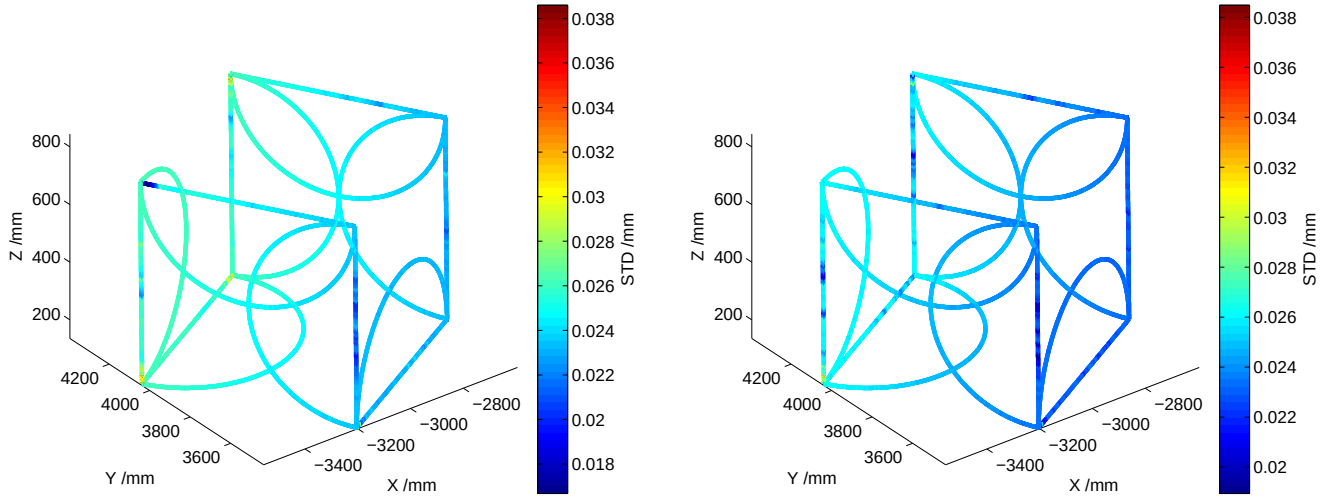

(a) Interacting Multiple Model (IMM) Filter

(b) Residual-Mean Interacting Multiple Model (RMIMM) Filter

Figure. 6. Hybrid systems analysis methods.

to determine if the RMIMM filter, in contrast to the more common IMM filter, could achieve its expected faster model detection. However, it was obvious that both hybrid system filters, in conjunction with the augmented measurement model, achieve a significantly better uncertainty estimation than a Kalman filter or manufacturers approximation can provide. In particular, the over shoots of the Kalman filter approach can be avoided, which makes the proposed approach suitable for more complex kinematic trajectories. Additionally, with the capabilities of the augmented measurement model to reflect local characteristics, it is possible to analyse the trajectory in a more appropriate way. Even if the proposed approach is also suitable for real-time applications, such as integration in a robot control loop, the sampling rate of the laser tracker must be considered.

The results reveal, that the alignment errors are more important than synchronisation errors if the delay time is relatively short. This effect is larger in a more far-range application. As the environmental conditions have a significant influence on an electromagnetic beam, it would be useful to have a time-varying refractive index to correct all readings of a laser tracker.

However, the analysis of a kinematically measured trajectory with Bayesian filtering, in conjunction with a hybrid system estimator, is a reasonable way to estimate and improve the uncertainty. However, it must be remembered that the internal system models must be roughly appropriate to the observed process.

VII. Outlook

Bayesian filters rely on the first-order Markov chain assumption which is invalid if there are systematic effects not taken into consideration. It is therefore necessary to generate a kinematic reference to test the measurement model with the objective of identifying additional, missing kinematic parameters which influence the system but are only noticeable at higher speeds.

A benefit of adopting Bayesian filters is that the new proposed approach is well suited for analyzing a trajectory which has been observed by more than one laser tracker. This sensor-fusion approach should lead to a significant lower trajectory uncertainty.

With regard to the coordinated turn model, it is possible here to calculate an approximation of the orientation angles. This approximation could be used to improve a 6 DOF estimation where Leica's T-Cam (6 DOF tracking accessory) cannot deliver readings because it has a measuring frequency of 100 Hz instead of the laser tracker's 1000 Hz.

References

[1] H. Kihlman, R. Loser, A. Cooke, A. Sunnanbo, and K. Von Arb, "Metrology-integrated industrial robots calibration, implementation and testing," in *International Symposium on Robotics (ISR)*, 2004.

[2] *emScon 3.5 Programmers Manual Tracker Programming Interface*, 3rd ed., Leica Geosystems AG, Leica Geosystems AG Metrology Division Mönchmattweg 5 5035 Unterentfelden Switzerland, August 2009.

[3] K. Foppe, V. Schwieger, and R. Staiger, "Grundlagen kinematischer mess- und auswertetechniken," in *Kinematische Messmethoden Vermessung in Bewegung*, 2004, pp. 3–18.

[4] R. Loser, *Weiterentwicklung eines absoluten, hochpräzisen und trackingfähigen Distanzmessers für industrielle Anwendungen*, ser. Mitteilungen. Institut für Geodäsie und Photogrammetrie an der Eidgenössischen Technischen Hochschule Zürich. Inst. für Geodäsie und Photogrammetrie, 2001.

[5] H. Kuhlmann, "Mathematische Modellbildung zu kinematischen prozessen," in *Kinematische Messmethoden Vermessung in Bewegung*, 2004, pp. 19–33.

[6] I. Hwang, H. Balakrishnan, and C. Tomlin, "State estimation for hybrid systems: applications to aircraft tracking," *Control Theory and Applications, IEE Proceedings* -, vol. 153, no. 5, pp. 556–566, Sep. 2006.

[7] S. Blackman and R. Popoli, *Design and analysis of modern tracking systems*, ser. Artech House radar library. Boston [u.a.]: Artech House, 1999, includes bibliographical references and index.

[8] Y. Bar-Shalom, X. R. Li, and T. Kirubarajan, *Estimation with applications to tracking and navigation : [theory, algorithms and software]*, ser. A Wiley-Interscience publication. New York: Wiley, 2001.

[9] X. Rong Li and V. P. Jilkov, "Survey of maneuvering target tarcking, part I: Dynamic models," *IEEE Transactions On Aerospace And Electronic Systems*, vol. 5428, no. 4, pp. 1333–1364, 2003.

[10] M. Althoff, "Reachability analysis and its application to the safety assessment of autonomous cars," Ph.D. dissertation, Technische Universität München, 2010.

[11] B. Ristic, S. Arulampalam, and N. Gordon, *Beyond the Kalman filter : particle filters for tracking applications*, ser. Artech House radar library. Boston, Mass. [u.a.]: Artech House, 2004.

[12] S. Thrun, W. Burgard, and D. Fox, *Probabilistic robotics*, ser. Intelligent robotics and autonomous agents. Cambridge, Mass.: MIT Press, 2005.

[13] N. Yang, W. Tian, and Z. Jin, "An interacting multiple model particle filter for manoeuvring target location," *Measurement Science and Technology*, vol. 17, no. 6, p. 1307, 2006.

[14] M. Montemerlo, S. Thrun, and B. Siciliano, *FastSLAM: a scalable method for the simultaneous localization and mapping problem in robotics*, ser. Springer tracts in advanced robotics. Springer, 2007.

[15] T. Emter and T. Ulrich, "Visuelle Information zur robusten Zuordnung von Landmarken für die Navigation mobiler Roboter," in *Forum Bildverarbeitung. Hrsg.: F. Puente León*, 2010, pp. 95–106.

[16] R. Loser, "Kinematische Messmethoden im industriellen Nahbereich," in *Kinematische Messmethoden Vermessung in Bewegung*, 2004, pp. 233–243.

[17] B. Muralikrishnan, D. Sawyer, C. Blackburn, S. Phillips, B. Borchardt, and W. T. Estler, "Asme b89.4.19 performance evaluation tests and geometric misalignments in laser trackers," *Journal Of Research Of The National Institute Of Standards And Technology*, vol. 114, no. 1, pp. 21–35, 2009.

[18] B. Hughes, A. Forbes, A. Lewis, W. Sun, D. Veal, and K. Nasr, "Laser tracker error determination using a network measurement," *Measurement Science and Technology*, vol. 22, no. 4, p. 045103, 2011.

[19] R. Loser and S. Kyle, "Alignment and field check procedures for the leica laser tracker ltd 500," in *Boeing Large Scale Optical Seminar*, 1998.

[20] R. Joeckel, M. Stober, and W. Huep, *Elektronische Entfernungs- und Richtungsmessung und ihre Integration in aktuelle Positionierungsverfahren*, 5th ed. Heidelberg: Wichmann, 2008.

[21] Jcgm, "Evaluation of measurement data supplement 1 to the guide to the expression of uncertainty in measurement propagation of distributions using a monte carlo method," *Evaluation*, vol. JCGM 101:2, no. September, p. 90, 2008.

[22] S. Dan, *Optimal state estimation : Kalman, H. [infinity] and nonlinear approaches*. Hoboken, NJ: Wiley-Interscience, 2006.

[23] H. W. Lilliefors, "On the kolmogorov-smirnov test for normality with mean and variance unknown," *Journal of the American Statistical Association*, vol. 62, no. 318, pp. 399–402, 1967.

[24] M. A. Stephens, "Edf statistics for goodness of fit and some comparisons," *Journal of the American Statistical Association*, vol. 69, no. 347, pp. 730–737, 1974.

[25] *Leica Laser Tracker System*, Leica Geosystems AG, Mönchmattweg 5 CH-5035 Unterentfelden (Switzerland), 1999, lTD500.

[26] T. Terboven, "Laser tracker specification," personal communication via email, August 2012, Hexagon Metrology GmbH.